


# Parameter identification of the KUKA LBR iiwa robot including constraints on physical feasibility

**Conference Paper****Author(s):**

Stürz, Yvonne R.; Affolter, Lukas M.; [Smith, Roy](#) 

**Publication date:**

2017-07

**Permanent link:**

<https://doi.org/10.3929/ethz-b-000237831>

**Rights / license:**

[In Copyright - Non-Commercial Use Permitted](#)

**Originally published in:**

IFAC-PapersOnLine 50(1), <https://doi.org/10.1016/j.ifacol.2017.08.1208>

**Funding acknowledgement:**

141853 - Digital Fabrication - Advanced Building Processes in Architecture (SNF)

## Parameter Identification of the KUKA LBR iiwa Robot Including Constraints on Physical Feasibility

Yvonne R. Stürz\*, Lukas M. Affolter, Roy S. Smith\*

\* Automatic Control Laboratory, Eidgenössische Technische Hochschule,  
Physikstrasse 3, 8092 Zürich, Switzerland  
(e-mail: {stuerzy, rsmith}@control.ee.ethz.ch, lukasa@student.ethz.ch)

**Abstract:** The newly released KUKA LBR iiwa 14 R820 robot stands for *intelligent industrial work assistant* (iiwa) and is, like its predecessor LBR IV, equipped with torque sensors in each joint, and can be controlled through a real-time interface. Although the dynamic model of the robot is not published by the manufacturer, its knowledge is indispensable for simulation and control based on the system model. This paper presents the identification of the minimal set of base parameters, as well as a consistent set of physical parameters for a rigid-link model of the KUKA LBR iiwa 14 R820 robot, including friction. The experiments on the robot are conducted based on optimized excitation trajectories. The physical parameters, which are required for stable dynamic simulations, are identified by solving a nonlinear optimization problem, where constraints are included to ensure physical feasibility. A validation and cross-validation in simulation and experiments show a very accurate representation of the robot's dynamics by the resulting models. As a result, both sets of identified parameters are given.

© 2017, IFAC (International Federation of Automatic Control) Hosting by Elsevier Ltd. All rights reserved.

**Keywords:** Robots manipulators, parameter identification, constrained parameters, robot dynamics, industrial robots

### 1. INTRODUCTION

More and more tasks in various sectors, as in medical care or domestic and industrial applications, are assisted by or completely transferred to robotic manipulators. Robots are also planned to be used in the future in the construction industry, where more complex goals should be accomplished, such as cooperative tasks. The KUKA LBR iiwa 14 R820 is especially suited for research in robotics, as it is accessible through a real-time interface named *Fast Robot Interface*, see KUKA Robot Group (2015b). Moreover, it is mainly designed for interactions with humans, and is therefore equipped with torque sensors after the gearbox of each actuated joint, which allows for cooperative interaction control. In order to develop model-based controllers for a robotic manipulator, its dynamic model is needed. Furthermore, if complex multi-robot tasks are considered, it is valuable to do dynamic simulations of the robots' motions and interactions. In order to obtain reliable simulation results, it is again crucial to know the robot's model parameters.

In Bargsten et al. (2013), the identification of the dynamic parameters of the KUKA LBR IV, the predecessor of the LBR iiwa, is considered, and an identification procedure is outlined, but no parameters are published. Its dynamic parameters are published in Jubien et al. (2014b), and other approaches for the identification of the parameters used by KUKA for the LBR IV are proposed in Jubien et al. (2014a) and in Gaz et al. (2014). Although the LBR iiwa and its predecessor are similar, their dimensions are slightly different, and their parameters are not identical. In Besset et al. (2016), a method for static calibration of the geometric parameters of the LBR iiwa is proposed, but

to the best of our knowledge, no dynamic model parameters are currently publicly available for the KUKA LBR iiwa 14 R820.

In Albu-Schäffer and Hirzinger (2001) and Ott (2008), models for robots with flexible links are considered, which include joint elasticity and damping. However, as the joint stiffness of the KUKA LBR iiwa is very high, despite its torque sensors, a model of rigid links is used in this paper. Its validity is confirmed by the high accuracy of the results. Rigid link models can be formulated in terms of a minimal set of dynamic parameters, the base parameters, see Gautier and Khalil (1990), which can be beneficial in some cases. However, for dynamic simulations, a consistent set of the robot's physical parameters are required. This is the case for the open-source robotics simulation software Gazebo, see Koenig and Howard (2004), gazebo.org (2015). Therefore, both the set of base parameters and the set of consistent physical parameters of the KUKA LBR iiwa 14 R820 robot are identified.

For the identification of base parameters, the inverse dynamics model is used, as the dynamic parameters enter it linearly, see Siciliano et al. (2010). In order to maximize the information about the parameters in the robot's motion, optimal excitation trajectories are designed, which are tracked by the robot in experiments. Based on the measured joint torques and positions, the resulting equations, which are linear in the unknown parameters, are solved through a least-squares approach. To obtain physical parameters, which are usable in dynamic simulations, the identified parameters need to be physically consistent, as shown in Mata et al. (2005). Therefore, constraints are included in the identification, resulting in a nonlinear optimization problem. The resulting physical parameters are thus physically feasible and consistent with the robot's dynamics. However, they do not necessarily match reality, when there are more physical parameters than degrees of freedom in the dynamics. But a

\* This research was supported by the NCCR Digital Fabrication, funded by the Swiss National Science Foundation (NCCR Digital Fabrication Agreement # 51NF40-141853).

consistent set of parameters is obtained, which is suitable for reproducing the exact robot dynamics in stable simulations.

This paper is organized as follows. Section 2 states the equations of motion and the inverse dynamics model. In Section 3, the identification of the physical parameters is given as a nonlinear optimization problem. Section 4 gives experimental results and Section 5 concludes the paper. The identified base parameters and physical parameters are given in the Appendix.

## 2. DYNAMIC MODEL OF THE ROBOT

### 2.1 Equations of Motion

Despite the compliance due to its torque sensors, the KUKA LBR robot can be accurately modelled with rigid links. The equations of motion, as in Siciliano et al. (2010), are given by

$$\tau = B(q)\ddot{q} + C(q, \dot{q})\dot{q} + g(q) + F_v\dot{q} + F_s\text{sign}(\dot{q}), \quad (1)$$

where  $q, \dot{q}, \ddot{q} \in \mathbb{R}^n$ , with  $n$  the number of joints of the robot, are the vectors of joint position, velocities and accelerations, respectively.  $B(q) \in \mathbb{R}^{n \times n}$  is the inertia matrix,  $C(q, \dot{q})\dot{q}$  is the vector of torques due to centrifugal and coriolis effects and  $g(q)$  is the gravity vector.  $F_v$  and  $F_s \in \mathbb{R}^{n \times n}$  are diagonal matrices of the viscous and coulomb friction parameters. The terms in (1) depend on the configuration and motion of the robot, and on its physical parameters, which we stack for each link  $i$  in the vector

$$\mu_i := [m_i, l_{C_{ix}}, l_{C_{iy}}, l_{C_{iz}}, I_{ixx}, I_{ixy}, I_{ixz}, I_{iyy}, I_{iyz}, I_{izz}, F_{iv}, F_{is}]^T, \quad (2)$$

where  $m_i$  is the mass of link  $i$ , the vector  $[l_{C_{ix}}, l_{C_{iy}}, l_{C_{iz}}]^T$  defines the distance from the center of the  $i$ -th link frame to the center of mass of link  $i$ . The parameters  $I_{ixx}, I_{ixy}, I_{ixz}, I_{iyy}, I_{iyz}$  and  $I_{izz}$  form the symmetric inertia tensor of link  $i$ , defined relative to the center of mass of link  $i$  in the  $i$ -th link frame, as

$$I_i^i := \begin{bmatrix} I_{ixx} & I_{ixy} & I_{ixz} \\ * & I_{iyy} & I_{iyz} \\ * & * & I_{izz} \end{bmatrix}.$$

$F_{iv}$  and  $F_{is}$  are the parameters for viscous and coulomb friction, respectively. All physical parameters of the robot form the stacked vector  $\mu := [\mu_1^T, \dots, \mu_n^T]^T$ . Note that we neglect the kinetic and potential energy from the joint actuators, as their contributions are low in relation to the energy of the links, and no measurements of the rotors' angular velocity are available.

### 2.2 Inverse Dynamics Model (IDM)

For the identification of the dynamic model of rigid robots, the so-called inverse dynamics model is used. The dynamics equations are expressed linearly w.r.t. a set of dynamic parameters, which are stacked in the vector  $\pi = [\pi_1^T, \dots, \pi_n^T]^T$ , where for each link  $i$ ,  $i = 1, \dots, n$ , the parameter vector  $\pi_i$  is defined as

$$\pi_i := [M_i, MX_i, MY_i, MZ_i, XX_i, XY_i, XZ_i, YY_i, YZ_i, ZZ_i, FV_i, FS_i]^T. \quad (3)$$

The relationship between the dynamic parameters in (3) and the physical parameters in (2) are given by

$$\begin{aligned} M_i &:= m_i, & XX_i &:= I_{ixx} + m_i \cdot (l_{C_{iy}}^2 + l_{C_{iz}}^2), \\ MX_i &:= m_i \cdot l_{C_{ix}}, & XY_i &:= I_{ixy} - m_i \cdot l_{C_{ix}} \cdot l_{C_{iy}}, \\ MY_i &:= m_i \cdot l_{C_{iy}}, & XZ_i &:= I_{ixz} - m_i \cdot l_{C_{ix}} \cdot l_{C_{iz}}, \\ MZ_i &:= m_i \cdot l_{C_{iz}}, & YY_i &:= I_{iyy} + m_i \cdot (l_{C_{ix}}^2 + l_{C_{iz}}^2), \\ FV_i &:= F_{iv}, & YZ_i &:= I_{iyz} - m_i \cdot l_{C_{iy}} \cdot l_{C_{iz}}, \\ FS_i &:= F_{is}, & ZZ_i &:= I_{izz} + m_i \cdot (l_{C_{ix}}^2 + l_{C_{iy}}^2). \end{aligned} \quad (4)$$

The inverse dynamics model is derived from the Lagrangian equations, as in Siciliano et al. (2010), and is given by

$$\underbrace{\begin{bmatrix} \tau_1 \\ \tau_2 \\ \vdots \\ \tau_n \end{bmatrix}}_{\tau} = \underbrace{\begin{bmatrix} y_{11}^T & y_{12}^T & \dots & y_{1n}^T \\ 0^T & y_{12}^T & \dots & y_{1n}^T \\ \vdots & \vdots & \ddots & \vdots \\ 0^T & 0^T & \dots & y_{nn}^T \end{bmatrix}}_{Y(q, \dot{q}, \ddot{q})} \cdot \underbrace{\begin{bmatrix} \pi_1 \\ \pi_2 \\ \vdots \\ \pi_n \end{bmatrix}}_{\pi}. \quad (5)$$

The matrix  $Y$  can be computed from measurements of  $q$  and estimates of  $\dot{q}$  and  $\ddot{q}$ .

### 2.3 Reduction to Base Parameters

Depending on the kinematic structure, the complete set of dynamic parameters is not required to uniquely specify the robot's motion, see Gautier and Khalil (1988). Therefore, the set of parameters to be identified can be reduced to a minimal set of parameters, as shown in Gautier and Khalil (1990), which are referred to as base parameters,  $\pi_b$ . The relationship between the complete vector of dynamic parameters,  $\pi$ , and the vector of base parameters,  $\pi_b$ , is linear. Details about the regrouping can be found in Khalil and Dombre (2004). The equations for regrouping  $\pi$  to  $\pi_b$ , for the KUKA LBR iiwa, with  $n = 7$ , are

$$\begin{aligned} ZZR_1 &:= ZZ_1 + YY_2, \\ MYR_2 &:= MY_2 + MZ_3 + rl_3 \cdot MR_3, \\ XXR_2 &:= XX_2 - YY_2 + YY_3 + 2 \cdot rl_3 \cdot MZ_3 + rl_3^2 \cdot MR_3, \\ ZZR_2 &:= ZZ_2 + YY_3 + 2 \cdot rl_3 \cdot MZ_3 + rl_3^2 \cdot MR_3, \\ MR_3 &:= M_3 + MR_4, & XXR_3 &:= XX_3 - YY_3 + YY_4, \\ MYR_3 &:= MY_3 + MZ_4, & ZZR_3 &:= ZZ_3 + YY_4, \\ MR_4 &:= M_4 + MR_5, \\ MYR_4 &:= MY_4 - MZ_5 - rl_5 \cdot MR_5, \\ XXR_4 &:= XX_4 + YY_5 - YY_4 + 2 \cdot rl_5 \cdot MZ_5 + rl_5^2 \cdot MR_5, \\ ZZR_4 &:= ZZ_4 + YY_5 + 2 \cdot rl_5 \cdot MZ_5 + rl_5^2 \cdot MR_5, \\ MR_5 &:= M_5 + MR_6, & MYR_6 &:= MY_6 + MZ_7, \\ MYR_5 &:= MY_5 - MZ_6, & XXR_6 &:= XX_6 - YY_6 + YY_7, \\ XXR_5 &:= XX_5 - YY_5 + YY_6, & MR_6 &:= M_6 + M_7, \\ ZZR_5 &:= ZZ_5 + YY_6, & ZZR_6 &:= ZZ_6 + YY_7, \\ XXR_7 &:= XX_7 - YY_7. \end{aligned} \quad (6)$$

The inverse dynamics model from (5) with  $\pi_b$  thus becomes

$$\tau = Y_b(q, \dot{q}, \ddot{q})\pi_b, \quad (7)$$

where the observation matrix  $Y$  from (5) is transformed into  $Y_b$ , according to the linear regrouping transformation of (6).

## 3. METHODS FOR DYNAMIC IDENTIFICATION

### 3.1 Least-Squares Approach

The dynamic model identification is based on the measurements of joint torques,  $\tau_{meas}$ , and joint positions,  $q_{meas}$ , of the robot during dynamic experiments. The joint velocities and accelerations,  $\dot{q}_{meas}$  and  $\ddot{q}_{meas}$ , respectively, are computed from the measurements. From this data, the matrix  $Y_b(q_{meas}, \dot{q}_{meas}, \ddot{q}_{meas})$  in (7) can be constructed, see Siciliano et al. (2010). During the experiment,  $M$  measurements along the trajectory are recorded. The  $m$ -th measurement is denoted by  $q_{meas}(m)$ . The resulting matrix equation is given by

$$\underbrace{\begin{bmatrix} \tau_{meas}(1) \\ \vdots \\ \tau_{meas}(M) \end{bmatrix}}_{\bar{\tau}_{meas}} = \underbrace{\begin{bmatrix} Y_b(q_{meas}(1), \dot{q}_{meas}(1), \ddot{q}_{meas}(1)) \\ \vdots \\ Y_b(q_{meas}(M), \dot{q}_{meas}(M), \ddot{q}_{meas}(M)) \end{bmatrix}}_{\bar{Y}_b} \pi_b + \underbrace{\begin{bmatrix} v(1) \\ \vdots \\ v(M) \end{bmatrix}}_{\bar{v}}, \quad (8)$$

with  $\bar{\tau}_{meas}$  the stacked vector of measured joint torque vectors. The vector  $\bar{v}$  contains the stacked measurement noise vectors  $v(m)$ , which are assumed to be additive zero mean Gaussian. In order to reconstruct the robot's motion, the reduced set of base parameters,  $\pi_b$ , can be estimated by solving the following least-squares optimization problem, see Bargsten et al. (2013),

$$\pi_{b,LS}^* := \underset{\pi_b}{\operatorname{argmin}} \|\bar{v}\|_2^2 = \underset{\pi_b}{\operatorname{argmin}} \|\bar{Y}_b \pi_b - \bar{\tau}_{meas}\|_2^2. \quad (9)$$

In order to reduce high-frequency noise, the measured data is filtered. Details about the data acquisition and measurement treatment are given in Section 4. The base parameters, which are obtained as the solution of (9), are sufficient to uniquely describe the robot's dynamics.

### 3.2 Consideration of Physical Feasibility

To obtain consistent physical parameters, a slightly different approach than solving (9) has to be taken. The identification is now formulated as an optimization problem in the physical parameters,  $\mu$ . The relation between the measured torques  $\tau$  and  $\mu$  is described by the observation matrix  $Y$  as in (5) and by the nonlinear relationship between  $\pi$  and  $\mu$  as defined in (4) and denoted by  $\pi(\mu)$ . In order to guarantee a physically meaningful result, constraints on the physical parameters  $\mu$  are introduced, leading to the following nonlinear optimization problem

$$\min_{\mu} \|\bar{\tau} - \bar{Y}\pi(\mu)\|_2^2 \quad (10a)$$

$$\text{s. t. } \mu_{lb} \leq \mu \leq \mu_{ub}, \quad (10b)$$

$$0 < m_i, \quad 0 < \operatorname{eig}(I_i^j), \quad (10c)$$

$$h(I_i^j) \leq 0, \quad \forall i \in \{1, \dots, n\}, \quad (10d)$$

where the lower and upper bounds  $\mu_{lb}$  and  $\mu_{ub}$  are taken from measurements, estimates, and CAD-files, see KUKA Robot Group (2015a). The constraints (10c) guarantee physical feasibility, i.e., positive masses and positive definite inertia tensors, see Mata et al. (2005). The constraints (10d) on the entries of the inertia matrix are introduced to obtain physical parameters compatible with Gazebo. They are in part documented in gazebosim.org (2014), and in part heuristically set to enable numerically stable simulations. The constraints (10d) are

$$\begin{aligned} [I_{izz}, I_{iyy}, I_{ixx}]^T - [I_{ixx} + I_{iyy}, I_{ixx} + I_{izz}, I_{iyy} + I_{izz}]^T &\leq 0, \\ \max(I_{ixx}, I_{iyy}, I_{izz}) - 100 \cdot \min(I_{ixx}, I_{iyy}, I_{izz}) &\leq 0, \\ 3[I_{jzz}, I_{kyy}]^T - [\min(I_{jxx}, I_{jyy}), \min(I_{kxx}, I_{kzz})]^T &\leq 0, \\ \max(|I_{ixy}|, |I_{ixz}|, |I_{iyz}|) - 0.1 \min(I_{ixx}, I_{iyy}, I_{izz}) &\leq 0, \\ -[I_{ixx}, I_{iyy}, I_{izz}]^T + 10^{-4}[1, 1, 1]^T &\leq 0, \\ -F_{iv} + 0.1 &\leq 0, \\ \forall i \in \{1, \dots, 7\}, \quad \forall j \in \{1, 3, 5\}, \quad \forall k \in \{2, 4\}. \end{aligned}$$

They impose the triangular inequality of the diagonal elements of the inertia matrix, see gazebosim.org (2014) and prevent big differences between them. Moreover, the smallest diagonal term of the inertia of links one to five is forced to correspond to the axis parallel to the link length. The non-diagonal elements of the inertia matrix should be small compared to the diagonal ones. Finally, lower bounds on the diagonal inertia elements and on the viscous friction coefficients are imposed.

Table 1. MDH Param. KUKA LBR iiwa 14 R820

Link $i$	$\gamma_i$	$\alpha_i$	$d_i$	$\theta_i$	$rl_i$	Link $i$	$\gamma_i$	$\alpha_i$	$d_i$	$\theta_i$	$rl_i$
1	0	0	0	$q_1$	0	5	0	$\pi/2$	0	$q_5$	0.40m
2	0	$\pi/2$	0	$q_2$	0	6	0	$\pi/2$	0	$q_6$	0
3	0	$-\pi/2$	0	$q_3$	0.42m	7	0	$-\pi/2$	0	$q_7$	0
4	0	$-\pi/2$	0	$q_4$	0						

### 3.3 Optimal Excitation Trajectories

In order to reduce errors in the least-squares solution of (9) due to measurement noise, the observation matrix needs to be well-conditioned. This is the case, if the robot's motion along the trajectories sufficiently excites the effect of the dynamic parameters, as the observation matrix  $\bar{Y}_b$  contains enough information for the parameter identification. To this end, we design optimal excitation trajectories to be tracked by the robot. The optimality criterion to be minimized is the condition number of  $\bar{Y}_b$ , referred to as  $\operatorname{cond}(\bar{Y}_b)$ , which is defined as the ratio between its largest and smallest singular values, see Gautier and Khalil (1991). The following parametrized Fourier series are chosen as excitation trajectories, see Bargsten et al. (2013),

$$q_i(t) := \sum_{l=1}^L \frac{a_{i,l}}{\omega_f^l} \sin(\omega_f l t) - \frac{b_{i,l}}{\omega_f^l} \cos(\omega_f l t), \quad i = 1, \dots, n, \quad (12)$$

for each joint  $i$ , where  $L$  is the number of sine- and cosine-terms and  $f_f = \frac{\omega_f}{2\pi}$  is the fundamental frequency. Thus, the joint velocities and accelerations can be analytically differentiated. The parameters of the Fourier series,  $a_{i,l}$  and  $b_{i,l}$ , are optimized with respect to the maximal information content of  $\bar{Y}_b$ , which is expressed by the optimization problem

$$\min_{a_{i,l}, b_{i,l}} \operatorname{cond}(\bar{Y}_b), \quad \forall i = \{1, \dots, n\}, \quad \forall l = \{1, \dots, L\}, \quad (13)$$

subject to physical constraints of the robot's kinematics and to its actuation limits, see KUKA Robot Group (2015c). Different approaches to the parametrized excitation trajectories are possible and were tested, such as sine series, splines, polynomials, but the Fourier series give the best result, i.e., the lowest condition number for  $\bar{Y}_b$ . The details of this optimization problem and the resulting optimal excitation trajectories applied to the KUKA LBR iiwa 14 R820 are given in Section 4.

## 4. EXPERIMENTS ON THE KUKA LBR IIWA

### 4.1 Description of the Robot's Kinematics

The KUKA LBR iiwa is a serial robot with  $n = 7$  rotational joints, and no translational degrees of freedom. Its structure is depicted in Figure 1. After each of the gearboxes, there are joint torque sensors. Moreover, the robot is equipped with joint position encoders, see KUKA Robot Group (2015c). Because of the serial structure, the kinematics can efficiently be described by the Modified Denavit-Hartenberg (MDH) convention, as in Khalil and Dombre (2004). The rotational axis of joint  $i$  is denoted by  $z_i$ , and the common normal axis between  $z_i$  and  $z_{i-1}$  is denoted by  $x_i$ . The parameter  $\gamma_i = 0$  indicates that joint  $i$  is a revolute joint,  $\alpha_i$  denotes the angle between the axes  $z_{i-1}$  and  $z_i$  about  $x_{i-1}$ .  $\theta_i$  is the angle between  $x_{i-1}$  and  $x_i$  about  $z_i$ . Finally,  $rl_i$  indicates the distance between the axes  $x_{i-1}$  and  $x_i$  along  $z_i$ . The MDH parameters of the KUKA LBR iiwa 14 R820 robot are given in Table 1. For the dynamic description of the robot, twelve physical parameters per link  $i$ ,  $\mu_i \in \mathbb{R}^{12}$  as in (2), can be defined. Alternatively, twelve dynamic parameters per link  $i$ ,  $\pi_i \in \mathbb{R}^{12}$  as in (3), can be used. The reduction to a minimal set

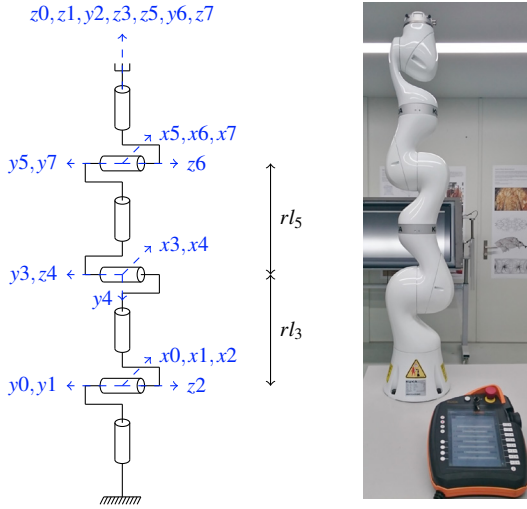


Fig. 1. Link frames of the KUKA LBR iiwa 14 R820

of parameters, as described in Section 2, leads to  $N_p = 57$  base parameters  $\pi_b$ , as detailed in Table 2 in the Appendix.

#### 4.2 Optimal Excitation Trajectories for the KUKA LBR iiwa

In the following, optimization problem (13) is solved in order to find the optimal excitation trajectories for the dynamic identification of the iiwa 14 R820. In the parametrized Fourier series (12), the number of sine- and cosine-terms is set to  $L = 5$  and the fundamental frequency to  $f_f = \frac{\omega_f}{2\pi} = 0.1$  Hz. The duration of the trajectory is 10 s and together with a sample frequency of 100 Hz, this leads to 1000 samples to construct the observation matrix  $\bar{Y}_b$ . The resulting optimization problem becomes

$$\min_{a_{i,l}, b_{i,l}} \text{cond}(\bar{Y}_b) \quad (14a)$$

$$\text{s. t. } q_i(t) := \sum_{l=1}^L \frac{a_{i,l}}{\omega_f l} \sin(\omega_f l t) - \frac{b_{i,l}}{\omega_f l} \cos(\omega_f l t), \quad (14b)$$

$$\left[ \sum_{l=1}^5 \frac{a_{i,l}}{l}, \sum_{l=1}^5 b_{i,l}, \sum_{l=1}^5 l \cdot a_{i,l} \right]^\top = 0, \quad (14c)$$

$$\sum_{l=1}^5 \frac{1}{l} \sqrt{a_{i,l}^2 + b_{i,l}^2} \leq \omega_f q_{i,\max}, \quad (14d)$$

$$\sum_{l=1}^5 \sqrt{a_{i,l}^2 + b_{i,l}^2} \leq \dot{q}_{i,\max}, \quad (14e)$$

$$[a_{i,l} \ b_{i,l}]^\top \leq \min \left( l \cdot \frac{2\pi}{5T_f} q_{i,\max}, \dot{q}_{i,\max} \right) [1 \ 1]^\top, \quad (14f)$$

$$-[a_{i,l} \ b_{i,l}]^\top \leq -\max \left( l \cdot \frac{2\pi}{5T_f} q_{i,\min}, \dot{q}_{i,\min} \right) [1 \ 1]^\top, \quad (14g)$$

$$\forall i = 1, \dots, 7, \quad \forall l = 1, \dots, 5,$$

where  $q_{i,\min}$ ,  $q_{i,\max}$  and  $\dot{q}_{i,\min}$ ,  $\dot{q}_{i,\max}$  are the lower and upper bounds on the joint positions and velocities of the robot, respectively. They can be found in KUKA Robot Group (2015c). The constraints (14c)-(14e) account for zero initial joint positions, velocities and accelerations of the trajectories. In order to achieve a feasible trajectory, bounds on the parameters  $a_{i,l}$  and  $b_{i,l}$  are set in (14f)-(14g). In Figure 2, the optimal trajectories  $q_i^*(t)$  for the joints  $i = 1, \dots, 7$  are depicted, which give a condition number of  $\text{cond}(\bar{Y}_b) = 65$ . In Figure 3, the resulting path of the end-effector during the optimal trajectory is shown.

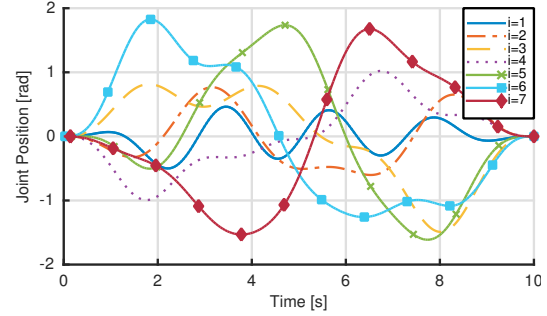


Fig. 2. Position trajectories of the seven joints during excitation.

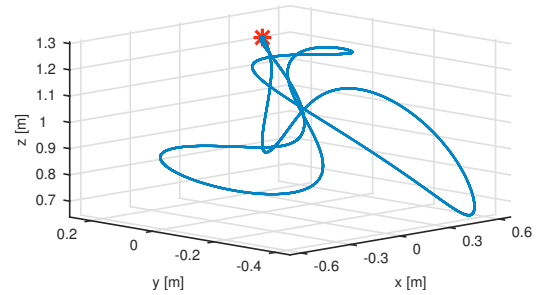


Fig. 3. Cartesian position of the end-effector during the excitation trajectory, \* denotes the start and end position.

#### 4.3 Experimental Data Acquisition

The optimal excitation trajectories  $q_i^*(t)$ ,  $i = 1, \dots, 7$ , for the seven joints are commanded in the *Joint Position Control Mode* from the real-time client *Fast Robot Interface* to the robot, see KUKA Robot Group (2015b). The joint positions and torques from the robot are recorded with a sampling frequency of  $f_s = 1$  kHz over  $K = 16$  periods. The raw recorded data is denoted by  $\tilde{q}_{meas}$  and  $\tilde{\tau}_{meas}$ , for the joint positions and torques, respectively. The  $m$ -th measurements are denoted by  $\tilde{q}_{meas}(m)$  and  $\tilde{\tau}_{meas}(m)$  and are averaged over the  $K$  recorded periods according to  $\tau_{meas}(m) := \frac{1}{K} \sum_{k=1}^K \tilde{\tau}_{meas,k}(m)$ ,  $q_{meas}(m) := \frac{1}{K} \sum_{k=1}^K \tilde{q}_{meas,k}(m)$ , with  $\tilde{q}_{meas,k}$  and  $\tilde{\tau}_{meas,k}$  being the recorded data from period  $k$ . The measured and averaged joint positions  $q_{meas}(m)$ , with  $m = 1, \dots, M$ , are then filtered offline with a non-causal zero-phase low-pass IIR Butterworth filter of order 20 and of a cutoff frequency of 2 Hz in both the forward and the reverse direction. This filtering approach can be found in Gautier et al. (2013). From the resulting data, the joint velocities and accelerations are estimated using a central difference algorithm to avoid lag. The measured and averaged joint torques  $\tau_{meas}(m)$  are filtered in the same way with a low-pass IIR Butterworth filter of order 12 and of a cutoff frequency of 1.6 Hz. With this processed data,  $\bar{\tau}_{meas} = [\tau_{meas}(1), \dots, \tau_{meas}(M)]^\top$  and  $\bar{Y}_b(q_{meas}, \dot{q}_{meas}, \ddot{q}_{meas})$  are computed as in (8).

#### 4.4 Estimation of Base Parameters

Using the averaged and filtered measurements of the joint torques  $\tau_{meas}(m)$  and joint positions  $q_{meas}(m)$  and the computed estimates of the joint velocities and accelerations  $\dot{q}_{meas}(m)$  and  $\ddot{q}_{meas}(m)$ , the observation matrix  $\bar{Y}_b$  is computed and the least-squares optimization problem (9) is solved. The results of the identified base parameters are given in Table 2 in the Appendix, together with their relative standard deviations, which are indicators of the quality of the individual parameter estimates, see Khalil and Dombre (2004), computed by  $\sigma_{\pi_{j,i}\%} =$



$100(\sigma_{\pi_j}/|\pi_j|)$ , with  $\sigma_{\pi_j} := \sqrt{C_{\pi}(j, j)}$  being the standard deviation of the estimation error of the parameter  $j$ ,  $j = 1, \dots, N_p$ , with  $N_p$  the number of base parameters and

$$C_{\pi} := \sigma_{\rho}^2 (\bar{Y}^T \bar{Y})^{-1}, \quad (15)$$

the variance-covariance matrix of the estimation error. In (15), the variance of the parameter estimation,  $\sigma_{\rho}^2$ , is computed, as in Khalil and Dombre (2004), by  $\sigma_{\rho}^2 := \|\bar{\tau} - \bar{Y}\pi\|_2^2 / (Mn - N_p)$ . The standard deviations indicate very accurate results for all parameters except joint seven. One reason for this is that its mass and absolute range of torques are much smaller compared to the other joints, necessarily leading to bigger relative standard deviations for the same absolute deviations. However, whereas the accuracy of the parameters of lower joints in the kinematic chain is important, as the motions of higher joints depend on them, this is not the case for the seventh joint. It could in fact be controlled without relying on its model parameters, by a simple feedback controller. A further validation of the identified base parameters is presented in Section 4.6.

#### 4.5 Estimation of Consistent Physical Parameters

In order to obtain a consistent set of physical parameters, the nonlinear optimization problem (10a)-(10d) is solved using the SQP solver of fmincon in Matlab. The initial values are chosen based on approximations of the robot's links as cylinders of homogeneous mass distribution. The results of the identified consistent physical parameters of the KUKA LBR iiwa 14 R820 are given in Table 3 in the Appendix.

#### 4.6 Validation and Cross-Validation of the Identified Parameters

In order to test the quality of the estimated parameters, four reference trajectories  $q_{ref,j}(t)$ ,  $j = 1, \dots, 4$ , are defined and a comparison is done between the joint torques  $\bar{\tau}_{meas}$  which are measured in experiments on the robot tracking the reference trajectories and the joint torques  $\bar{\tau}_{sim}$  which are computed, *simulated*, using the dynamic model with the identified parameters in Matlab. As a quantifier, the root mean square error between the measured and simulated torques of joint  $i$  is computed according to  $\epsilon_{RMS,i} := \sqrt{\frac{1}{M} \sum_{m=1}^M (\tau_{meas,i}(m) - \tau_{sim,i}(m))^2}$ . For a direct validation, the excitation trajectory of the identification is used as the first reference trajectory,  $q_{ref,1}(t) = q^*(t)$ , with  $q^*(t)$  solving (14a)-(14g). The resulting RMS values for the identified base parameters and physical parameters are given in Table 4 in the Appendix. Both are in the same range and indicate a very high precision of the identified sets of parameters. The RMS values for the base parameters are slightly smaller, as they represent the global optimum of (9), whereas the physical parameters could represent a local optimum of (10a)-(10d) because of the nonlinearity of the problem.

For the validation of the physical parameters, the joint torques are also simulated in Gazebo. All three time series of the joint torques, i.e. the measured ones, and the simulated ones in Matlab and Gazebo, are shown in Figure 4. In Gazebo, in order to ensure good reference tracking, an inverse dynamics PD-controller is used, which neglects friction. This is a reason for the higher deviations between the measured values and the simulated values in Gazebo in comparison to the deviations between the measured torques and the simulated ones in Matlab.

To do a cross-validation of the identified physical parameters, another three reference trajectories different from the excitation

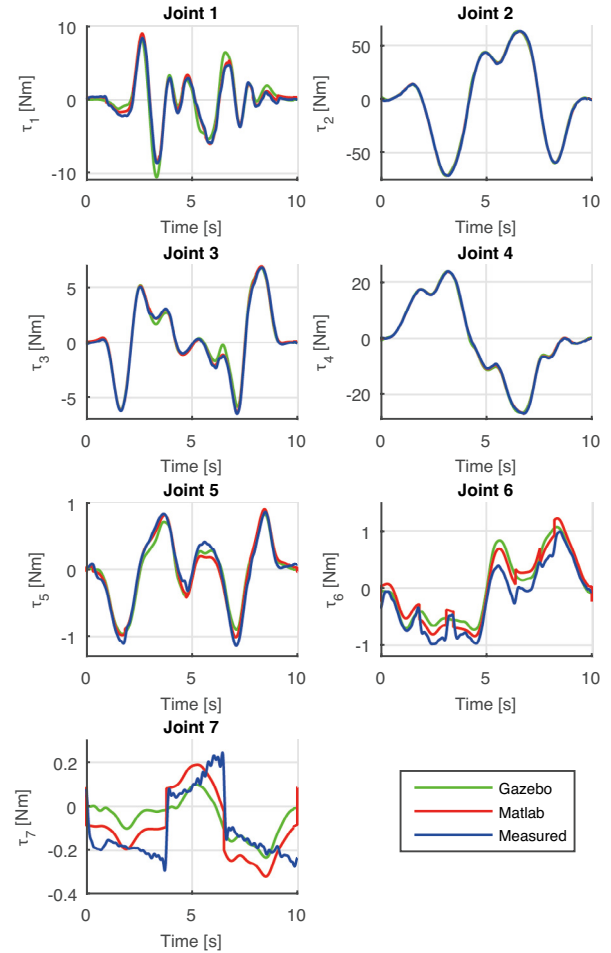


Fig. 4. Joint torques during parameter validation using reference trajectory  $q_{ref,1}(t)$ : Simulated and measured values.

trajectory are used. The second one,  $q_{ref,2}(t)$ , is defined as a sine series trajectory  $q_{ref,2,i}(t) := \sum_{l=1}^L a_{i,l} \sin(b_{i,l}t)$ ,  $i = 1, \dots, 7$ , with  $L = 5$  and where the parameters  $a_{i,l}, b_{i,l}$  are optimized for the excitation of the robot's parameters, in the same way as in (14a)-(14g). The third reference trajectory,  $q_{ref,3}(t)$ , is defined as a fifth order polynomial trajectory. It is defined through  $k = 1, \dots, K$  with  $K = 10$  intervals of random durations  $T^k$ . At the end of the intervals, randomly defined waypoints  $D_i^k$  have to be reached by joint  $i$ ,  $i = 1, \dots, 7$ . The part of the trajectory for joint  $i$  between the two way points  $k-1$  and  $k$  is defined as

$$q_{ref,3,i}^k(t) = \left( 10 \cdot \left( \frac{t}{T^k} \right)^3 - 15 \cdot \left( \frac{t}{T^k} \right)^4 + 6 \cdot \left( \frac{t}{T^k} \right)^5 \right) \cdot D_i^k + D_i^{k-1}.$$

The total duration of  $q_{ref,3}(t)$  is  $\sum_{k=1}^K T^k = 10$  s. The fourth reference trajectory  $q_{ref,4}(t)$  is defined similarly to  $q_{ref,3}(t)$ ; it is again a fifth order polynomial trajectory, but is defined by  $K = 20$  instead of 10 random intervals. The total duration is again  $\sum_{k=1}^K T^k = 10$  s. The resulting RMS-errors between the measured torques and the simulated ones using Matlab for the cross-validation with all three reference trajectories  $q_{ref,2}(t)$ ,  $q_{ref,3}(t)$  and  $q_{ref,4}(t)$  are given in Table 4 in the Appendix.

## 5. CONCLUSION

The minimal set of base parameters as well as a consistent set of physical parameters of the KUKA LBR iiwa 14 R820 robot have been identified in experiments with optimal excitation tra-

jectories. Both sets of parameters give a correct description of the robot's dynamics. A direct validation and cross-validation of the identified parameters in simulations and experiments show a very good match to the dynamic model of the robot. The knowledge of a consistent set of physical parameters is very useful for stable dynamic simulations.

## ACKNOWLEDGEMENTS

The authors would like to thank Prof. Philippe Block, ETH Zürich, for providing the experimental facilities.

## REFERENCES

- Albu-Schäffer, A. and Hirzinger, G. (2001). Parameter Identification and Passivity Based Joint Control for a 7 DOF Torque Controlled Light Weight Robot. In *Int. Conf. Robotics and Automation (ICRA)*, 2852–2858.
- Bargsten, V., Zometa, P., and Findeisen, R. (2013). Modeling, Parameter Identification and Model-Based Control of a Lightweight Robotic Manipulator. In *IEEE Int. Conf. Contr. Applications (CCA)*, 134–139.
- Bessey, P., Olabi, A., and Gibaru, O. (2016). Advanced calibration applied to a collaborative robot. In *2016 IEEE Int. Power Electronics and Motion Contr. Conf. (PEMC)*, 662–667. doi:10.1109/EPEPMC.2016.7752073.
- Gautier, M., Janot, A., and Vandanjon, P.O. (2013). A New Closed-Loop Output Error Method for Parameter Identification of Robot Dynamics. *IEEE Trans. Contr. Sys. Techn.*
- Gautier, M. and Khalil, W. (1988). On the Identification of the Inertial Parameters of Robots. In *27th Conf. Decis. Contr.*
- Gautier, M. and Khalil, W. (1990). Direct Calculation of Minimum Set of Inertial Parameters of Serial Robots. *IEEE Trans. Robotics and Automation*, 368–373.
- Gautier, M. and Khalil, W. (1991). Exciting Trajectories for the Identification of Base Inertial Parameters of Robots. In *30th IEEE Conf. Decis. Contr.*, 494–499.
- Gaz, C., Flacco, F., and de Luca, A. (2014). Identifying the Dynamic Model Used by the KUKA LWR: A Reverse Engineering Approach. In *IEEE Inter. Conf. Robotics and Automation (ICRA)*, 1386–1392.
- gazebosim.org (2014). Find Out Inertial Parameters. <http://gazebosim.org/tutorials>.
- gazebosim.org (2015). Gazebo. <http://gazebosim.org>.
- Jubien, A., Gautier, M., and Janot, A. (2014a). Dynamic Identification of the KUKA Light Weight Robot: Comparison Between Actual and Confidential KUKA's Parameters. In *IEEE/ASME Int. Conf. Adv. Intell. Mechatronics*.
- Jubien, A., Gautier, M., and Janot, A. (2014b). Dynamic Identification of the KUKA LWR Robot using Motor Torques and Joint Torque Sensor Datas. In *19th IFAC World Congress*.
- Khalil, W. and Dombre, E. (2004). *Modeling, Identification and Control of Robots*. Kogan Page Science, London.
- Koenig, N. and Howard, A. (2004). Design and Use Paradigms for Gazebo, An Open-Source Multi-Robot Simulator. In *Int. Conf. Intell. Robots and Sys.*, 2149–2154.
- KUKA Robot Group (2015a). KUKA Download Center CAD. <http://www.kuka-robotics.com>.
- KUKA Robot Group (2015b). *KUKA Sunrise.Connectivity FRI 1.7*. Augsburg, Germany, 1st edition.
- KUKA Robot Group (2015c). *LBR iiwa 7 R800, LBR iiwa 14 R820 Specification*. Augsburg, Germany, 5th edition.
- Mata, V., Benimeli, F., Farhat, N., and Valera, A. (2005). Dynamic Parameter Identification in Industrial Robots considering physical Feasibility. *Advanced Robotics*, 19, 101–119.
- Ott, C. (2008). *Modeling of Flexible Joint Robots*, 13–27. Springer, Berlin, Heidelberg.
- Siciliano, B., Sciavicco, L., Villani, L., and Oriolo, G. (2010). *Robotics: Modelling, Planning and Control*. Springer Verlag, London.

## APPENDIX

Table 2. Identified base parameters  $\pi_b$  and relative standard deviation  $\sigma$ .

Par.	Value	$\sigma$ [%]	Par.	Value	$\sigma$ [%]	Par.	Value	$\sigma$ [%]
ZZR <sub>1</sub>	-0.146	1.02	FV <sub>3</sub>	0.144	2.65	FS <sub>5</sub>	0.085	2.81
FV <sub>1</sub>	0.181	2.15	FS <sub>3</sub>	0.083	3.02	MX <sub>6</sub>	-0.005	3.62
FS <sub>1</sub>	0.336	0.69	MX <sub>4</sub>	-0.006	4.26	MYR <sub>6</sub>	0.097	0.20
MX <sub>2</sub>	-0.020	2.98	MYR <sub>4</sub>	-2.272	0.02	XXR <sub>6</sub>	-0.007	12.43
MYR <sub>2</sub>	5.805	0.01	XXR <sub>4</sub>	0.751	0.30	XY <sub>6</sub>	-0.020	2.69
XXR <sub>2</sub>	2.361	0.19	XY <sub>4</sub>	-0.009	11.51	XZ <sub>6</sub>	0.009	4.90
XY <sub>2</sub>	0.033	4.15	XZ <sub>4</sub>	-0.005	17.66	YZ <sub>6</sub>	0.021	2.07
XZ <sub>2</sub>	-0.025	7.19	YZ <sub>4</sub>	0.020	5.07	ZZR <sub>6</sub>	0.009	6.17
YZ <sub>2</sub>	0.022	7.29	ZZR <sub>4</sub>	0.780	0.19	FV <sub>6</sub>	0.137	1.87
ZZR <sub>2</sub>	2.280	0.12	FV <sub>4</sub>	0.070	6.29	FS <sub>6</sub>	0.102	2.09
FV <sub>2</sub>	0.356	1.19	FS <sub>4</sub>	0.207	1.14	MX <sub>7</sub>	-0.004	5.78
FS <sub>2</sub>	0.161	1.58	MX <sub>5</sub>	0.005	5.35	MY <sub>7</sub>	0.001	24.84
MX <sub>3</sub>	-0.025	2.87	MYR <sub>5</sub>	0.081	0.41	XXR <sub>7</sub>	-0.015	3.33
MYR <sub>3</sub>	0.018	2.16	XXR <sub>5</sub>	0.021	7.64	XY <sub>7</sub>	-0.000	167.21
XXR <sub>3</sub>	0.048	6.35	XY <sub>5</sub>	0.029	2.35	XZ <sub>7</sub>	-0.003	12.96
XY <sub>3</sub>	-0.038	3.66	XZ <sub>5</sub>	-0.025	2.33	YZ <sub>7</sub>	0.007	5.47
XZ <sub>3</sub>	-0.054	2.90	YZ <sub>5</sub>	0.008	9.40	ZZR <sub>7</sub>	-0.020	3.16
YZ <sub>3</sub>	-0.022	7.21	ZZR <sub>5</sub>	-0.002	42.25	FV <sub>7</sub>	0.008	31.49
ZZR <sub>3</sub>	0.051	2.87	FV <sub>5</sub>	0.040	6.77	FS <sub>7</sub>	0.166	1.31

Table 3. Identified physical parameters with constraints for physical feasibility and Gazebo.

Par.	Link 1	Link 2	Link 3	Link 4	Link 5	Link 6	Link 7
$m_i$	3.94781	4.50275	2.45520	2.61155	3.41000	3.38795	0.35432
$l_{C_{ix}}$	-0.00351	-0.00767	-0.00225	0.00020	0.00005	0.00049	-0.03466
$l_{C_{iy}}$	0.00160	0.16669	-0.03492	-0.05268	-0.00237	0.02019	-0.02324
$l_{C_{iz}}$	-0.03139	-0.00355	-0.02652	0.03818	-0.21134	-0.02750	0.07138
$I_{ixx}$	0.00455	0.00032	0.00223	0.03844	0.00277	0.00050	0.00795
$I_{ixy}$	0.00000	0.00000	-0.00005	0.00088	-0.00001	-0.00005	0.00022
$I_{ixz}$	-0.00000	0.00000	0.00007	-0.00112	0.00001	-0.00003	-0.00029
$I_{iyy}$	0.00454	0.00010	0.00219	0.01144	0.00284	0.00281	0.01089
$I_{iyz}$	0.00001	-0.00000	0.00007	-0.00111	-0.00000	-0.00004	-0.00029
$I_{izz}$	0.00029	0.00042	0.00073	0.04988	0.00012	0.00232	0.00294
$F_{iv}$	0.24150	0.37328	0.11025	0.10000	0.10000	0.12484	0.10000
$F_{is}$	0.31909	0.18130	0.07302	0.17671	0.03463	0.13391	0.08710

Table 4. RMS Errors between measured and simulated torques for joints  $i$  in Matlab.  $q_{ref,1}(t)$ : validation of  $\pi_b$  and  $\mu$ .  $q_{ref,2}(t)$ ,  $q_{ref,3}(t)$  and  $q_{ref,4}(t)$ : cross-validation of the physical parameters  $\mu$ .

joint	$\pi_b$	$\mu$	$\mu$	$\mu$	$\mu$
	$q_{ref,1}(t)$	$q_{ref,2}(t)$	$q_{ref,3}(t)$	$q_{ref,4}(t)$	
	RMS [Nm]	RMS [Nm]	RMS [Nm]	RMS [Nm]	RMS [Nm]
$i = 1$	0.29	0.35	0.34	0.55	0.43
$i = 2$	0.36	0.39	0.44	0.48	0.74
$i = 3$	0.13	0.14	0.23	0.23	0.15
$i = 4$	0.15	0.17	0.17	0.25	0.27
$i = 5$	0.08	0.09	0.12	0.15	0.06
$i = 6$	0.18	0.21	0.22	0.22	0.15
$i = 7$	0.06	0.10	0.12	0.12	0.06
Total	1.25	1.44	1.64	2.0	1.87